

Optimisation of Zinc Oxide Nanoparticle Biosynthesis Using *Saccharomyces Cerevisiae* with Box-Behnken Design

FITRY MULYANI, M. DIKI PERMANA, SAFRI ISHMAYANA, IMAN RAHAYU, DIANA RAKHMAWATY EDDY*

Universitas Padjadjaran, Faculty of Mathematics and Natural Sciences, Department of Chemistry, Sumedang, West Java 45363, Indonesia

Abstract: Zinc oxide nanoparticles have wide applications as catalysts, antimicrobial agents, drug delivery agents, etc. because of their intrinsic properties. Various methods can be applied to synthesise nanoparticles, one of which is the biosynthesis process. Biosynthesis is more eco-friendly than chemical and physical methods. In the present study, the optimisation of zinc oxide nanoparticle biosynthesis using the yeast *Saccharomyces cerevisiae* was performed by applying a response surface method called the Box–Behnken design (BBD). Three factors were optimised in the present study, namely the concentration of zinc acetate as the precursor (X_1), concentration of the *S. cerevisiae* fermentation broth (X_2), and the incubation time (X_3). The mass of zinc oxide nanoparticles (Y) was recorded as the response of the experiment. The product was then characterised by fourier transform infrared spectroscopy (FTIR), X-Ray diffraction (XRD), scanning electron microscopy/energy dispersive spectroscopy (SEM/EDS), and particle size analyser (PSA). The optimum conditions for the preparation of zinc oxide nanoparticles were found to be 0.3 M, 100% (v/v), and 24 h as the zinc acetate concentration, medium concentration, and incubation time, respectively. The FTIR analysis showed peaks at $\sim 600\text{ cm}^{-1}$, which is characteristic for ZnO stretching. From the XRD result, the ZnO nanoparticles with hexagonal structure was confirm. The SEM/EDS analysis confirmed that the morphology was spherical and showed the major energy emission for zinc and oxygen. Moreover, the PSA analysis revealed that the smallest size was 218.6 nm (12%) when the synthesis was performed at the optimum conditions, while when the incubation time was prolonged for 120 h, the size decreased to 134.2 nm.

Keywords: Biosynthesis, Box-Behnken, *Saccharomyces cerevisiae*, ZnO nanoparticles

1. Introduction

Nanomaterials are very interesting because of their wide applications. Nanomaterials with small particle sizes and large surface areas have potential in various industrial fields such as food packaging industry [1], cosmetics [2], medicine [3], and catalysts [4]. One of the many studies carried out thus far is metal oxide nanoparticle preparation, such as zinc oxide (ZnO), titanium dioxide (TiO_2), and silver oxide (Ag_2O). ZnO nanoparticles have receive considerable attention because of their good conductivity, chemical stability, photonic and optoelectronic properties, and antibacterial, antifungal, and UV-filtering properties; therefore, they are considered for biological applications such as antimicrobial agents, drug delivery, and bioimaging probes [5], making ZnO nanoparticles interesting to synthesise.

Many studies to prepare nanoparticles have been carried out using physical, chemical, or biological methods, including co-precipitation [6], sol-gel [7], hydrothermal [8], microemulsion [9], biosynthesis [10], electrochemistry [11] and irradiation [12].

Biosynthesis is a biological method that is eco-friendly as compared to chemical and physical methods, which are dangerous and expensive [10]. Biosynthesis is more eco-friendly because the process does not use toxic solvents, high temperature, and high pressure and does not require a long reflux process [5,10]. Thus, biosynthesis can approach the green chemistry principle [5,19]. The synthesis of nanoparticles by using the biosynthesis method involves the use of microorganisms, enzymes, plants, and algae as a medium to form the nanoparticles [10]. Microorganisms such as yeast have a number of advantages, such as the ability to absorb and accumulate toxic metal ions in high concentrations from

*email: diana.rahmawati@unpad.ac.id



the environment. Yeast cells can adapt to toxic conditions by using various detoxification mechanisms, such as bio-precipitation, chelation and intracellular sequestration [13]. *Saccharomyces cerevisiae* (*S. cerevisiae*) is the best yeast species from the perspectives of physiology and genetics and is one of the choices in the synthesis of nanoparticles. *S. cerevisiae* is an excellent yeast used for the commercial-scale production of biological molecules because of its high fermentation capacity and safe organism [14].

Nowadays, a systematic assessment of multiple formulation variables needs to be carried out to achieve a better product [15]. Therefore, a statistical design experiment such as the response surface method (RSM) is used to optimise the biosynthesis process. RSM has been successfully applied to various optimisation procedures in the extraction process and in pharmaceutical research [16]. There are two types of RSM methods, namely central composite design (CCD) and Box–Behnken design (BBD) [17]. In this study, we used the BBD because of the relatively few experimental runs required, making BBD more efficient and effective than CCD [18].

The purpose of this study was to biosynthesise zinc oxide nanoparticles using *S. cerevisiae* and determine the optimum conditions to obtain the maximum mass of zinc oxide nanoparticles with BBD.

2. Materials and methods

2.1 Materials

Zinc acetate dihydrate (Merck KGaA), *S. cerevisiae* A18, bacteriological peptone (LP0037, Oxoid), ammonium sulphate (Merck KGaA), D-glucose (Merck KGaA), potassium dihydrogen phosphate (Merck KGaA), yeast extract (LP0021, Oxoid), and aquadest were used in this study. All of these materials were obtained from Germany and England.

2.2 Method

2.2.1 Experimental Design

BBD with three factors and three levels was used in this study (Table 1). The experiments were conducted using the Minitab 17 software. The concentration of zinc acetate dihydrate (X_1), the concentration of the fermentation broth (X_2) and the incubation time (X_3) were used as the independent variables, and the mass of ZnO was recorded as the experimental response (Y).

Table 1. Independent Variables and Their Levels in the Box–Behnken Design

Factor/Independent Variables	Low (-1)	Medium (0)	High (+1)
X_1 = Concentration of zinc acetate (M)	0.1	0.2	0.3
X_2 = Concentration of fermentation broth (%)	10	55	100
X_3 = Incubation time (h)	24	72	120

The total medium used was 100 mL (E.g.: 10% fermentation broth means 10 mL of fermentation broth and 90 mL of aquadest).

2.2.2 Preparation of yeast inoculum

The inoculum of *S. cerevisiae* A18 was prepared on the yeast extract peptone medium (0.5% yeast extract, 0.5% bacteriological peptone, 0.3% ammonium sulphate, 0.3% potassium dihydrogen phosphate, and 1% D-glucose dissolved in 100 mL of aquadest). The medium was sterilised using an autoclave (121°C, 15 min) and was used to grow the yeast after inoculation with the yeast stock culture and incubation for 24 h.

2.2.3 Zinc Acetate Solution Preparation

Zinc acetate dihydrate was dissolved in aquadest with varying concentrations of 0.1 M, 0.2 M, and 0.3 M.

2.2.4 Biosynthesis of Zinc Oxide Nanoparticles

The *S. cerevisiae* culture medium was centrifuged for 15 min (10,000 rpm), and the supernatant was used for the biosynthesis process. Zinc acetate solution was added into the flask containing the supernatant and the mixture was further incubated at room temperature at a shaking speed of 180 rpm. After the incubation, the solution was centrifuged, and the pellets were washed with aquadest several times and dried at 60-70°C.

2.2.5 Characterisation

The samples were characterised using FTIR (PerkinElmer Spectrum 100), XRD (D8 Bruker Advance with generator 40.0 kV and 35.0 kV at 25°C), SEM/EDS (SU3500, 3.00 kV) and PSA (Horiba Scientific SZ-100). The FTIR characterisation was performed using KBr as a blank. The samples for the PSA characterisation were measured in the colloidal state by using distilled water.

3. Results and discussions

3.1 ZnO Nanoparticle Preparation

The formation of ZnO nanoparticles was confirmed through a visual assessment. The colour of the reaction mixture changed from yellowish to pale yellowish during the reaction and white sediments were formed, indicating the formation of ZnO nanoparticles (Figure 1). ZnO nanoparticles have formed because of the interaction between the hydroxyl groups that have a negative charge from the amino acid and the Zn^{2+} ions [19]. Amino acid was assumed to act as a capping agent. The capping agent plays an important role in the process of nanoparticle formation by controlling the morphology and shape and preventing aggregation [20]. The synthesis of metal nanoparticles also depends on the existence of the reductase enzyme in the microbes. The mechanism of the biosynthesis of nanoparticles involves the reduction of Zn^{2+} ions by an enzymatic metal reduction process in the presence of a reducing medium. Microorganisms are known to secrete enzymes such as NADH and nitrate reductase. These enzymes were assumed to act as a reducing agent in the bioreduction process of the metal ions and the formation of nanoparticles [5].

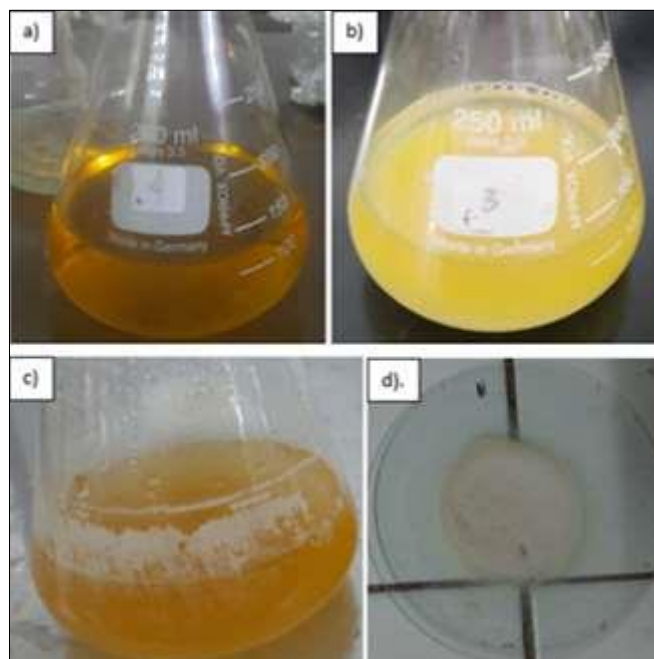


Figure 1. a) Fermentation broth, b) after addition of zinc acetate, c) after biosynthesis and d) product of biosynthesis process

3.2 Optimum Conditions for Biosynthesis of ZnO Nanoparticles

Through the experimental process, the mass of zinc oxide nanoparticles (g) as shown in Table 2, was collected as the response data (Y). The ANOVA result of this experiment showed a *P*-value of 0.002 (Figure 2) for the summary model analysis. From this analysis, we also obtained the following mathematical model:

$$Y = -0.0849 + 0.00354X_2 + 0.440X_1 + 0.00106X_3 - 0.000030X_{22} - 0.58X_{12} - 0.000002X_{32} + 0.01130X_2.X_1 - 0.000005X_2.X_3 - 0.00361X_1.X_3$$

Table 2. Results of optimisation of biosynthesis of ZnO nanoparticles

Run Order	Independent Variable			Response (Mass (g))	
	X_1 (M)	X_2 (%)	X_3 (h)	Theoretical	Practical
1	0.2	55	72	0.2023	0.2214
2	0.2	100	120	0.2117	0.2082
3	0.2	10	120	0.0407	0.0266
4	0.1	10	72	0.0334	0.0442
5	0.2	100	24	0.2549	0.2691
6	0.1	100	72	0.1243	0.1199
7	0.3	10	72	0.0456	0.0487
8	0.3	55	120	0.2207	0.2356
9	0.2	10	24	0.0407	0.0438
10	0.3	100	72	0.3399	0.3277
11	0.1	55	120	0.1415	0.1495
12	0.3	55	24	0.2770	0.2696
13	0.2	55	72	0.2023	0.1638
14	0.1	55	24	0.1284	0.1141
15	0.2	55	72	0.2023	0.2211

Analysis of Variance						
Source	DF	Adj SS	Adj MS	F-Value	P-Value	
Model	9	0.124783	0.013865	20.15	0.002	
Linear	3	0.098962	0.032987	47.94	0.000	
X_2	1	0.072485	0.072485	105.35	0.000	
X_1	1	0.025742	0.025742	37.41	0.002	
X_3	1	0.000735	0.000735	1.07	0.349	
Square	3	0.013797	0.004599	6.68	0.034	
X_2*X_2	1	0.013790	0.013790	20.04	0.007	
X_1*X_1	1	0.000126	0.000126	0.18	0.687	
X_3*X_3	1	0.000061	0.000061	0.09	0.778	
2-Way Interaction	3	0.012024	0.004008	5.83	0.044	
X_2*X_1	1	0.010343	0.010343	15.03	0.012	
X_2*X_3	1	0.000477	0.000477	0.69	0.443	
X_1*X_3	1	0.001204	0.001204	1.75	0.243	
Error	5	0.003440	0.000688			
Lack-of-Fit	3	0.001240	0.000413	0.38	0.784	
Pure Error	2	0.002200	0.001100			
Total	14	0.128224				

Figure 2. Results of model summary statistical analysis

Figure 2 shows that the independent variable that affected the response from the linear model was the concentration of zinc acetate and the concentration of the fermentation broth. From the square and the two-way interaction, these variables were determined to be the interaction of the fermentation broth and the interaction between the fermentation broth and zinc acetate, respectively. The P -value of the lack-of-fit was 0.784.

The ANOVA result of this experimental design showed a P -value of less than 0.05, implying that the hypothesis showed a real value; a P -value of >0.05 would indicate an insignificant value. From the analysis, we concluded that the linear, square, and two-way interaction model gave a real value (P -value < 0.05). If the P -value was less than 0.05, the mathematical model could have a significant effect on the response. The P -value of the lack-of-fit was greater than 0.05, confirming that the mathematical model could be accepted.

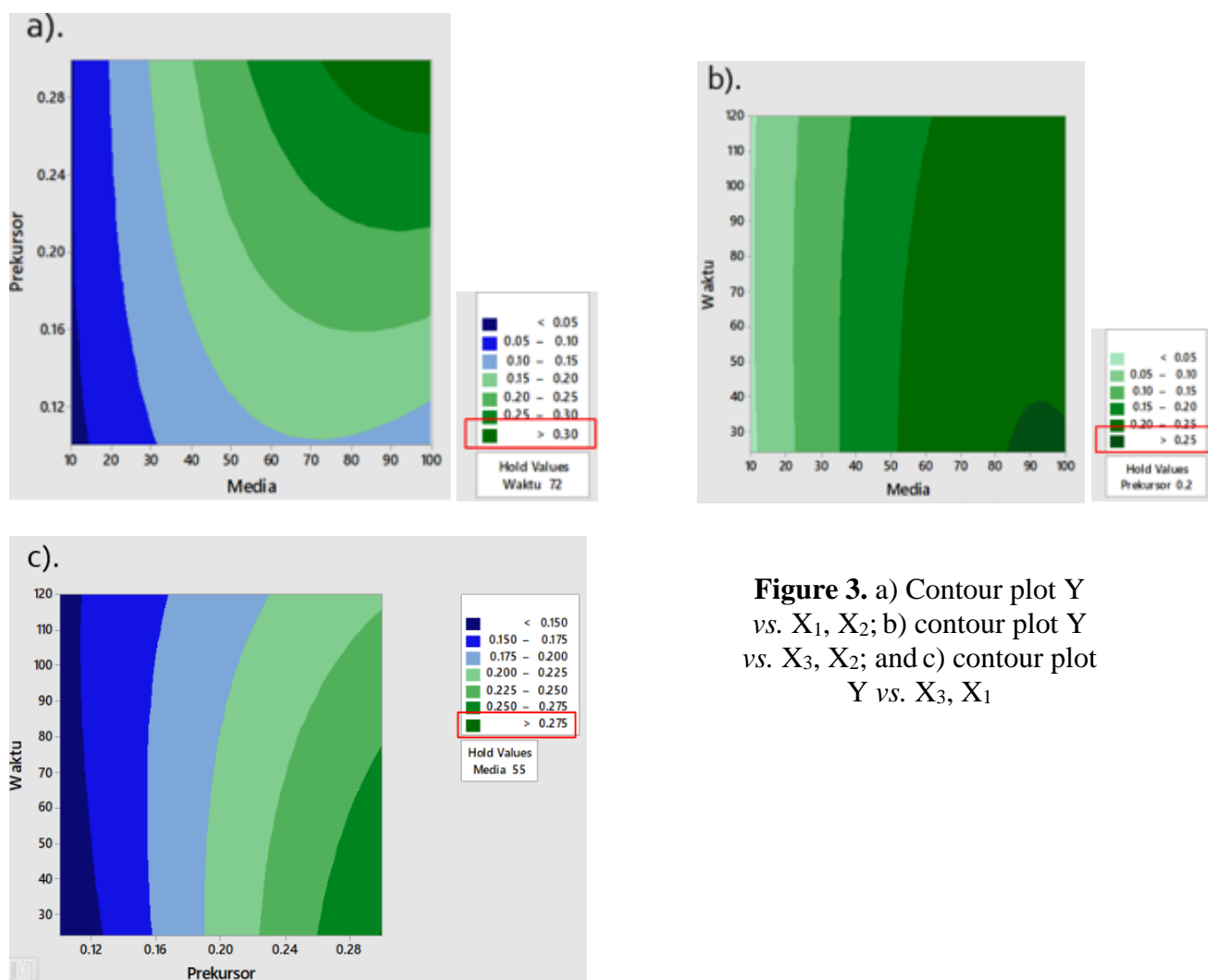


Figure 3. a) Contour plot Y vs. X_1 , X_2 ; b) contour plot Y vs. X_3 , X_2 ; and c) contour plot Y vs. X_3 , X_1

Figure 3 presents the contour plots of the mass of ZnO nanoparticles against the concentration of zinc acetate, the concentration of the fermentation broth and the incubation time, which show the stationary points in the dark green area. A stationary point in the dark green area indicates the optimum conditions to get a response (Y), which in this study was the maximum mass of the ZnO nanoparticles. Therefore, the maximum concentrations of zinc acetate and the fermentation broth (Figures 3a and b) and the minimum incubation time (Figures 3b and c) were the optimum conditions to get the maximum Y.

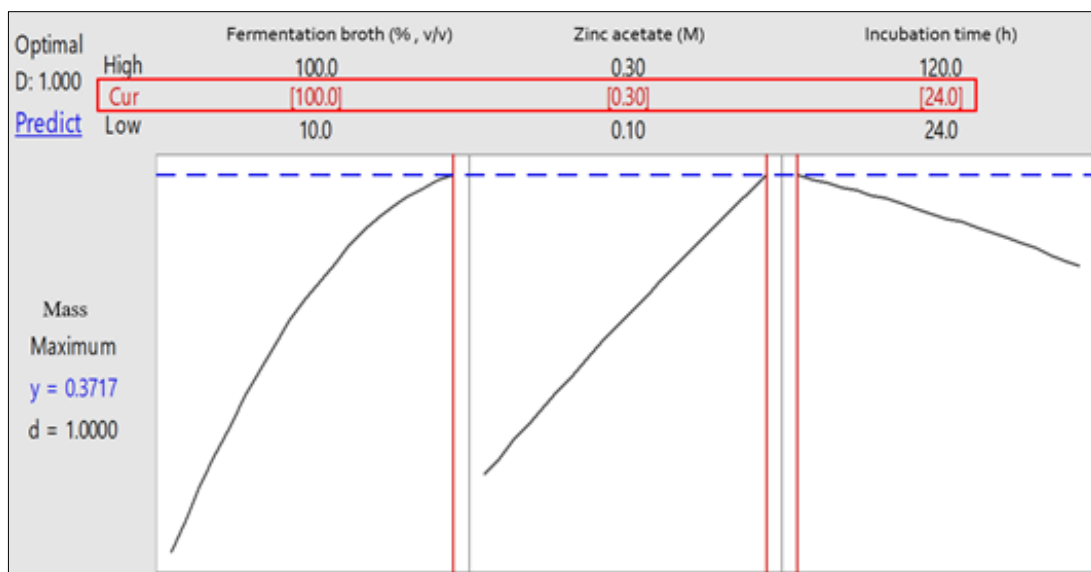


Figure 4. Results of optimum response of biosynthesis of ZnO nanoparticles

The optimum conditions for the concentration of zinc acetate, the concentration of the fermentation broth, and the incubation time were 0.3 M, 100%, 24 h, respectively (Figure 4). This result corresponded to the contour plot and the surface plot. Figure 4 also shows a desirability value (d) of 1.000, and the prediction of Y was 0.3717 g. The value of $d = 1$ indicated that the response was right on target, whereas if $d = 0$, then the response would have been outside the target [21]. The mathematical model was verified by running an experiment with the suggested optimum conditions. The experiment conducted under the optimum conditions gave 0.3289 ± 0.01 g, with an error percentage of $11.51\% \pm 2.69\%$. This was the maximum value obtained as compared to the other variations. Therefore, these results were compatible with the experimental design to obtain the maximum value of the response variable.

3.3 Fourier Transform Infrared (FTIR) Spectra

The FTIR spectra are presented in Figure 5. They confirmed the structure of the ZnO nanoparticles from the biosynthesis. The band that appeared at 3536 cm^{-1} (Figure 5a) corresponded to the NH group [22]. The bands at 3271.0 and 3321.0 cm^{-1} indicated the existence of a hydroxyl group from the phenolic compound. Other bands appeared at 1645 cm^{-1} , 1420.9 cm^{-1} , and $1114.6\text{--}1111.7\text{ cm}^{-1}$, confirming, respectively, the stretching vibration of C=C, bonding of CH_3 and the stretching vibration of C-C [23]. The band at $1026.9\text{--}1025.6\text{ cm}^{-1}$ showed the stretching vibration from C-O-C [24]. The bands at 634.8 and 635.5 cm^{-1} were correlated to the stretching vibration of ZnO nanoparticles. It appeared around this area probably because of the carbonate moieties that are generally observed when FTIR samples are measured in air [25].

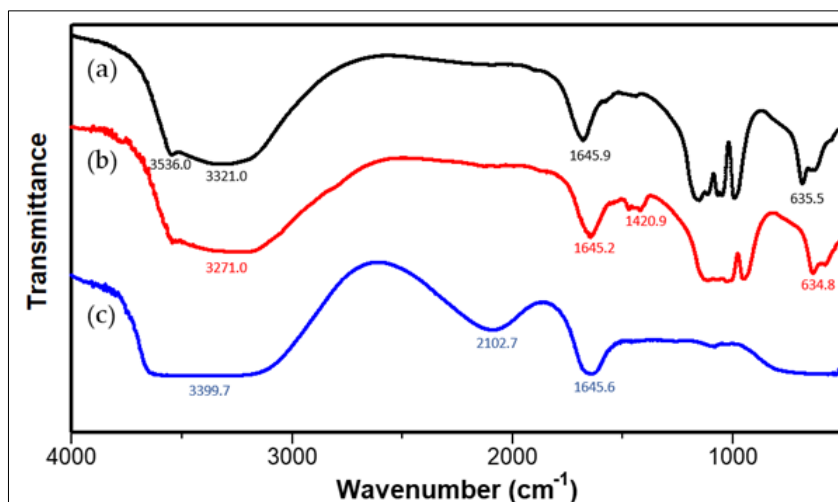


Figure 5. FTIR spectra of biosynthesis of ZnO nanoparticles with variation: a) 100%; 0.3 M; 120 h and b) 100%; 0.3 M; 24 h c) FTIR spectra of fermentation broth

The results of the FTIR analysis showed that bioactive functional groups such as hydroxyl and other functional groups still existed in the zinc oxide sample to achieve a stable state [23]. The existence of functional groups ($-\text{NH}_2$, $-\text{OH}$, $\text{C}=\text{O}$, $\text{C}-\text{O}-\text{C}$, $\text{C}-\text{N}-\text{C}$, and $-\text{S}-\text{S}-$) on the biosynthesis product was attributed to the secretion of metabolites such as amino acid, protein, and/or polysaccharide from *S. cerevisiae*. These metabolites were assumed to act as a capping agent by donating their electrons to the metal ions to form nanoparticles [19].

3.4 XRD Analysis

The XRD pattern of biosynthesis ZnO nanoparticles can be seen in Figure 6. The peaks from both XRD pattern of biosynthesis zinc oxide nanoparticles at 24 h (Figure 6c) and 120 h (Figure 6b) indicate the hexagonal crystal structure and existence of zincite crystal phase. Based on ICSD 98-065-6331 with crystalline planes (002), (012), (113) and (022) at 34°C , 50°C , 60°C and 77° respectively, indicate the hexagonal structure of ZnO nanoparticles. While crystalline planes (010), (002), (012), (110), and (013) at 31° , 35° , 46° , 54.5° and 61° respectively, indicate zincite crystal phase of ZnO nanoparticles based on ICSD 98-003-1060. The crystallinity of ZnO nanoparticles with incubation time 24 h was 51.3% and it increase to 55% after the incubation time was prolonged to 120h. Low crystallinity for both biosynthesis ZnO nanoparticles due to the processes is carried out at room temperature, whereas to get high crystallinity requires a high calcination temperature.

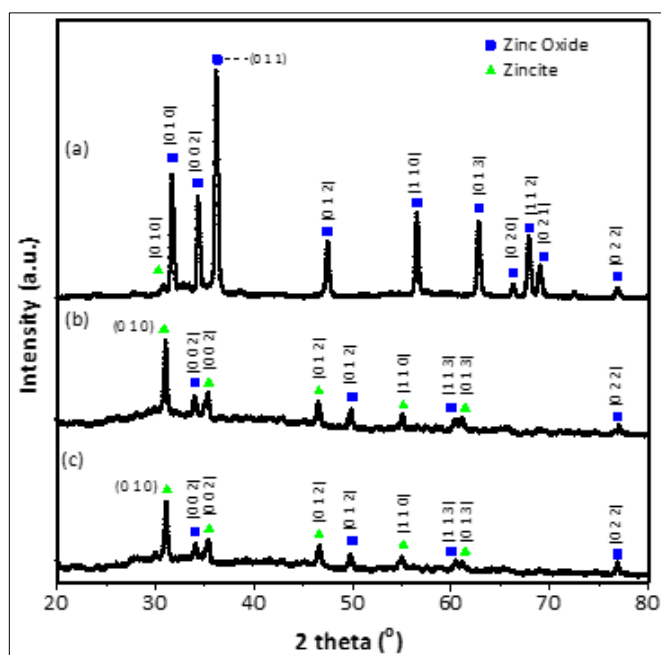


Figure 6. XRD pattern of
a) commercial ZnO and
biosynthesis ZnO
nanoparticles at
b) 120 h c) 24 h

3.5 SEM/EDS Analysis

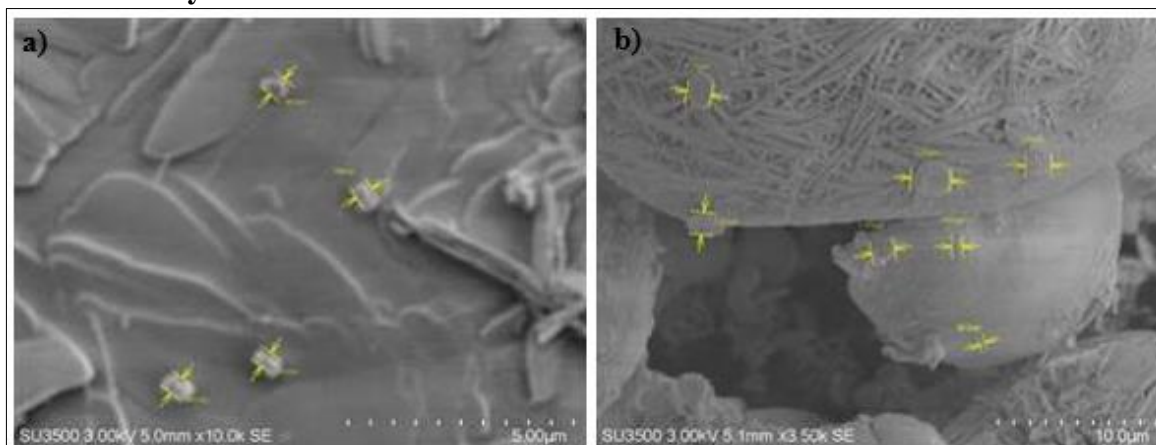


Figure 7. SEM analysis of biosynthesis of zinc oxide nanoparticles: a) 24 h and b) 120 h

The SEM analysis of the biosynthesis of zinc oxide nanoparticles is shown in Figure 7. The images show that the morphology was spherical, and when the incubation time was 120 h, the size of the nanoparticles formed was approximately 39.2 nm. Through the EDS analysis shown in Figure 8 and Table 3, we confirmed the presence of zinc oxide nanoparticles. This figure shows the major emission energies for zinc (51.22 and 50.77 wt%) and oxygen (27.76 and 26.15 wt%) for both incubation times. The other elements existed, such as carbon and nitrogen, because of the secretion of metabolites from *S. cerevisiae*. This corresponded to the peaks observed in the FTIR spectra.

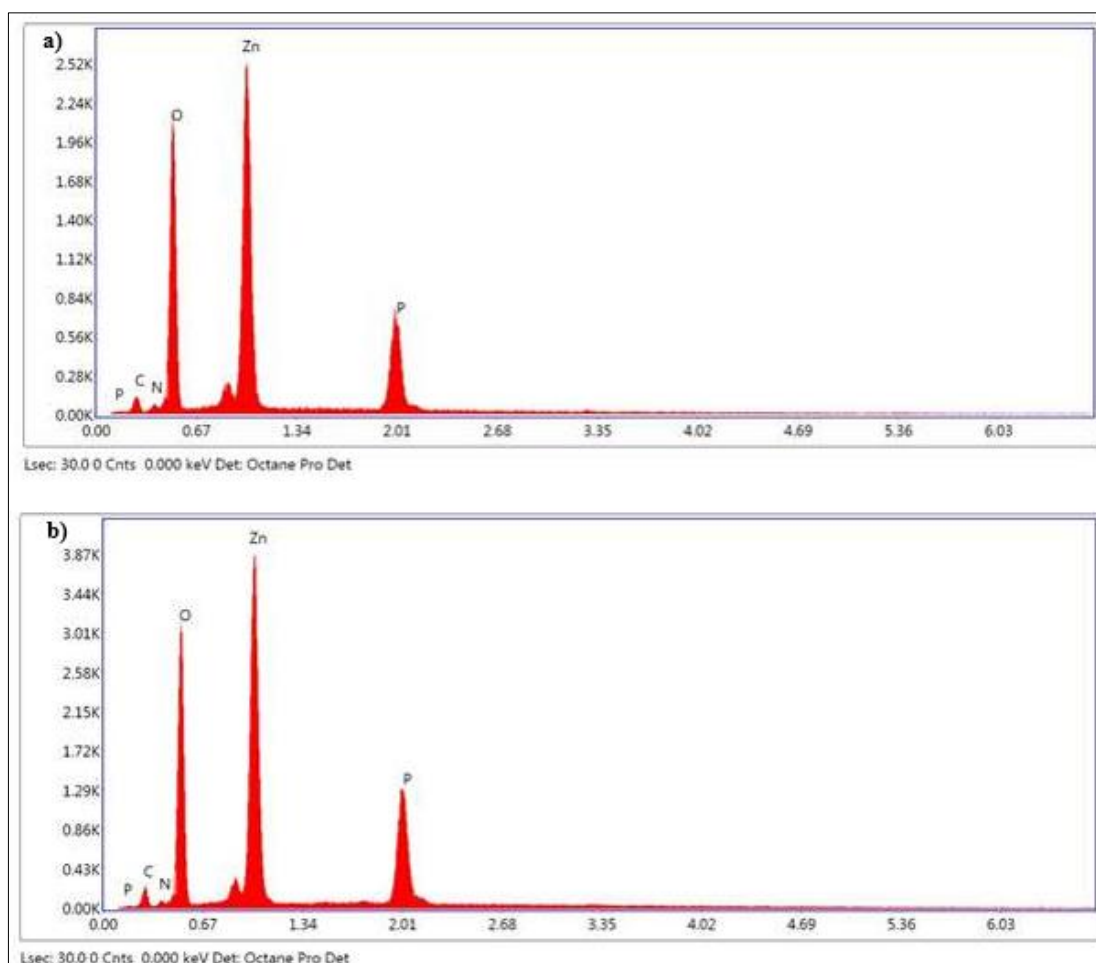


Figure 8. EDS analysis of biosynthesis of zinc oxide nanoparticles: a) 24 h and b) 120 h

Table 3. Percentage of emission energy biosynthesis ZnO nanoparticles

Element	Weight %		Atomic %	
	24 h	120 h	24 h	120 h
C	4.68	5.45	11.12	13.08
N	1.78	0.79	3.63	1.63
O	27.76	26.15	49.49	47.07
Zn	51.22	50.37	22.35	22.19
P	14.55	17.23	13.40	16.02

3.6 PSA Analysis

Two peaks were observed in the PSA analysis that used the dynamic light scattering (DLS) of the colloidal solution in both graphs (Figure 9). The aggregates were first revealed to have a diameter of approximately 218.6 nm when the incubation time was 24 h (Figure 9a). When this time was prolonged to 120 h (Figure 9b), the diameter decreased to 134.14 nm. The polydispersity index (PDI) also decreased from 0.846 to 0.809.

The PSA analysis showed that the incubation time affected the particle size: because of the nucleation rate and the interaction of metal ions with the capping agent, a longer incubation time led to a smaller particle size [19].

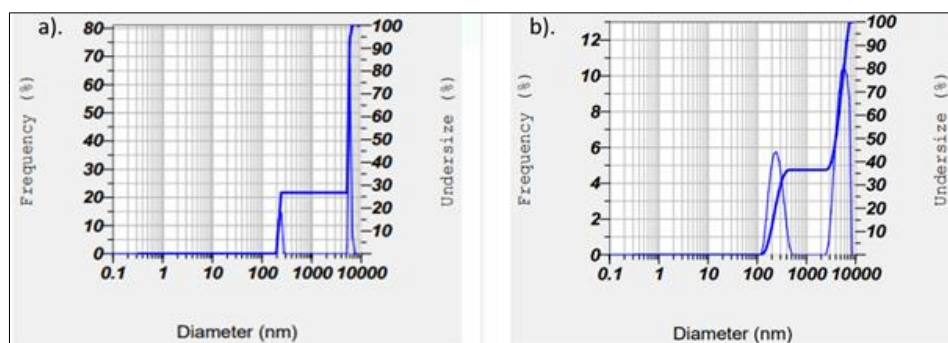


Figure 9. Particle size distribution analysis of biosynthesis of ZnO nanoparticles: a) 24 h and b) 120 h

4. Conclusions

The biosynthesis of ZnO nanoparticles was performed using *S. cerevisiae* as a bioreducing and capping agent as it is very eco-friendly and applies the green chemistry principle. The optimum conditions for obtaining the maximum amount of ZnO nanoparticles were determined using BBD. The optimum conditions were 0.3 M, 100% (v/v), and 24 h for the concentration of zinc acetate, the concentration of the fermentation broth, and the incubation time, respectively. The predicted mass of the nanoparticles formed under these conditions was 0.3717 g. From the XRD pattern, it was confirmed that the biosynthesis ZnO nanoparticles had a hexagonal structure. Through the SEM/EDS and PSA analysis, we confirmed that the incubation time affected the particle size. From the SEM/EDS, we confirmed that the morphology was spherical.

Acknowledgments: This research was supported by Ministry of Research and Technology, Republic of Indonesia, through PDUPT funding (grant no.: 1827/UN.3.1/LT/2020).

References

- JAYAKUMAR, A., K.V., H., T.S., S., JOSEPH, M., MATHEW, S., PRAVEEN, G., RADHAKRISHNAN E.K., Starch-PVA composite films with zinc-oxide nanoparticles and phytochemicals as intelligent pH sensing wraps for food package application, *Int. J. Biol. Macromol.*, **136**, 2019, 395-403.
- MOHAMMED, Y. H., HOLMES, A., HARIDASS, I. N., SANCHEZ, W. Y., STUDIER, H., GRICE, J. E., ROBERTS, M. S., Support for the Safe Use of Zinc Oxide Nanoparticle Sunscreens: Lack of Skin Penetration or Cellular Toxicity after Repeated Application in Volunteers, *J. Invest. Dermatol.*, **139**(2), 2019, 308-315.
- WU, B., WU, J., LIU, S., SHEN, Z., CHEN, L., ZHANG, X.-X., & REN, H., Combined effects of graphene oxide and zinc oxide nanoparticle on human A549 cells: Bioavailability, toxicity and mechanisms, *Environ. Sci. Nano*, **6**, 2019, 1594–1606.
- SHAMSUZZAMAN, MASHRAI, A., KHANAM, H., ALJAWF, R. N., Biological synthesis of ZnO nanoparticles using *C. albicans* and studying their catalytic performance in the synthesis of steroidal pyrazolines, *Arab J. Chem.*, **10**, 2017, S1530–S1536.
- CHAUHAN, R., REDDY, H., ABRAHAM, J., Biosynthesis of silver and zinc oxide nanoparticles using *Phicia fermentants* JA2 and their antimicrobial property, *Appl. Nanosci.*, **5**, 2015, 63-71.
- GANDHI, V., GANESAN, R., ABDULRAHMAN SYEDAHAMED, H. H., & THAIYAN, M., Effect of Cobalt Doping on Structural, Optical, and Magnetic Properties of ZnO Nanoparticles Synthesized by Coprecipitation Method, *J. Phys. Chem. C*, **118**(18), 2014, 9715–9725.
- BA-ABBAD, M. M., KADHUM, A. A. H., BAKAR MOHAMAD, A., TAKRIFF, M. S., & SOPIAN, K., The effect of process parameters on the size of ZnO nanoparticles synthesized via the sol-gel technique, *J. Alloys Compd.*, **550**, 2013, 63–70.
- RAI, P., & YU, Y. T. Citrate-assisted hydrothermal synthesis of single crystalline ZnO nanoparticles for gas sensor application. *Sensor Actuat. B-Chem.*, **173**, 2012, 58–65.



- 9.ZHANG, W., QIAO, X., CHEN, J., Synthesis of nanosilver colloidal particles in water/oil microemulsion, *Colloids Surf. A*, **299**, 2007, 22–28.
- 10.AZIZI, S., AHMAD, M. B., NAMVAR, F., MOHAMAD, R., Green biosynthesis and characterization of zinc oxide nanoparticle using brown marine macroalga *Sargassum muticum* aqueous extract, *Mater. Lett.*, **116**, 2014, 275-277.
- 11.MA, H., YIN, B., WANG, S., JIAO, Y., PAN, W., HUANG, S., Synthesis of silver and gold nanoparticles by a novel electrochemical method, *Chem Phys Chem*, **24**, 2004, 68–75.
- 12.EUTIS, S., KRYLOVA, G., EREMENKO, A., SMIRNOVA, N., SCHILL, A. W., EL-SAYED, M., Growth and fragmentation of silver nanoparticles in their synthesis with a fs laser and CW light by photo-sensitization with benzophenone, *Photochem. Photobiol. Sci.*, **4**, 2005, 154–159.
- 13.GAHLAWAT, G. & A. R. CHOUDHURY., A review on the biosynthesis of metal and metal salt nanoparticles by microbes, *RSC Adv.*, **9**, 2019, 12944–12967.
- 14.APEL, A. R., D'ESPAUX, L., WEHRS, M., SACHS, D., LIL, R. A., TONG, G. J., GARBER, M., NNADI, O., ZHUANG, W., HILLSON, N. J., KEASLING, J. D., MUKHOPADHYAY, A., A Cas9-based toolkit to program gene expression in *S.cerevisiae*, *Nucleic Acid Res.*, **45**(1), 2016, 496-508.
- 15.HAO, J., GAO, Y., ZHAO, J., ZHANG, J., LI, Q., ZHAO, Z., & LIU, J., Preparation and Optimization of Resveratrol Nanosuspensions by Antisolvent Precipitation Using Box-Behnken Design, *AAPS PharmSciTech*, **16**(1), 2014, 118–128.
- 16.DAS, A. K., & DEWANJEE, S., Optimization of extraction using mathematical models and computation, *Comput. Phytochem.*, 2018, 75-106.
- 17.WAGNER, J. R., MOUNT, E. M., & H.F., GILES., *Extrusion: The Definitive Processing Guide and Handbook*, William Andrew, USA, 2013, 291–308.
- 18.BA-ABBAD, M. M., CHAI, P. V., TAKRIFF, M. S., BENAMOR, A., MOHAMMAD, A. W., Optimization of nickel oxide nanoparticles synthesis through the sol gel method using Box–Behnken design, *Mater. Des.*, **86**, 2015, 948-956.
- 19.MOGHADDAM, A. B., MONIRI, M., AZIZI, S., RAHIM, R. A., ARIFF A. B., SAAD, W. Z., NAMVAR, F., NAVADERI, M., MOHAMMAD, R., Biosynthesis of ZnO Nanoparticles by a New *Phicia kudriavzevii* Yeast Strain and Evaluation of Their Antimicrobial and Antioxidants Activities, *Molecules*, **22**, 2017, 872.
- 20.SHARMA, D., KANCHI, S., & BISETTY, K., Biogenic synthesis of nanoparticles: A review, *Arab. J. Chem.*, **12**, 2019, 3576-3600.
- 21.MONTGOMERY, D.C. *Introduction to Statistical Quality Control* 6th Ed., John Wiley & Sons, New York, 2009.
- 22.SALARI, R., BAZZAZ, B. S. F., RAJABI, O., & KHASHYARMANESH, Z., New aspects of *Saccharomyces cerevisiae* as a novel carrier for berberine, *DARU J. Pharm. Sci.*, **21**, 2013, 73.
- 23.SRIRAMULU, M., & SUMATHI, S., Biosynthesis of palladium nanoparticles using *Saccharomyces cerevisiae* extract and its photocatalytic degradation behaviour, *Adv. Nat. Sci: Nanosci. Nanotechnol.*, **9**, 2018, 025018.
- 24.DOBRUCKA, R., & DUGASZEWSKA, J., Biosynthesis and antibacterial activity of ZnO nanoparticles using *Trifolium pratense* flower extract, *Saudi J. Biol. Sci.*, **23**, 2016, 517–523.
- 25.PREMANATHAN, M., KARTHIKEYAN, K., JEYASUBRAMANIAN, K., MANIVANNAN, G., Selective toxicity of ZnO nanoparticles toward Gram-positive bacteria and cancer cells by apoptosis through lipid peroxidation, *Nanomed. Nanotechnol. Biol. Med.*, **7**(2), 2011, 184–192.

Manuscript received: 16.11.2020